LASER INTERFEROMETER GRAVITATIONAL WAVE OBSERVATORY
- LIGO -
CALIFORNIA INSTITUTE OF TECHNOLOGY
MASSACHUSETTS INSTITUTE OF TECHNOLOGY

Document Type **LIGO-T970212-00 - D** 12/8/97

Mirror Thermoelastic Deflection in the LIGO Optical Surface Absorption Measurement System

D. Coyne

Distribution of this draft:

Detector

This is an internal working note
of the LIGO Project.

California Institute of Technology
LIGO Project - MS 51-33
Pasadena CA 91125
Phone (818) 395-2129
Fax (818) 304-9834
E-mail: info@ligo.caltech.edu

Massachusetts Institute of Technology
LIGO Project - MS 20B-145
Cambridge, MA 01239
Phone (617) 253-4824
Fax (617) 253-7014
E-mail: info@ligo.mit.edu

WWW: http://www.ligo.caltech.edu/

Abstract

Contamination of the high reflectance surfaces of the LIGO optics by outgassing in the vacuum system is a potentially significant problem. A resonant cavity method for testing the suitability of materials has been proposed[1]. This method relates the shift in the frequency of the cavity TEM_{01} (or TEM_{10}) mode as a function of recirculating power intensity, to a thermally induced radius of curvature change (ROC) due to surface absorption at the sub-ppm level. The purpose of this note is to relate the ROC change to surface absorptivity by thermoelastic analysis.

Keywords: thermal lensing, thermoelastic deflection, mirror contamination

1 RESONANT CAVITY GEOMETRY

The geometry of the resonant cavity used in the LIGO optical surface absorption measurement system is indicated in Figure 1. The Nd:YAG laser light (λ = 1.064 μm) is injected through one optic. The laser frequency is controlled to track the cavity length by the reflection locking technique. The cavity is suspended on two thin wire loops in a ultra-high vacuum system.

Figure (1) LIGO optical surface absorption measurement system resonant cavity geometry. The cavity is suspended by two wire loops in a vacuum chamber (p ~ 10^{-6} torr)

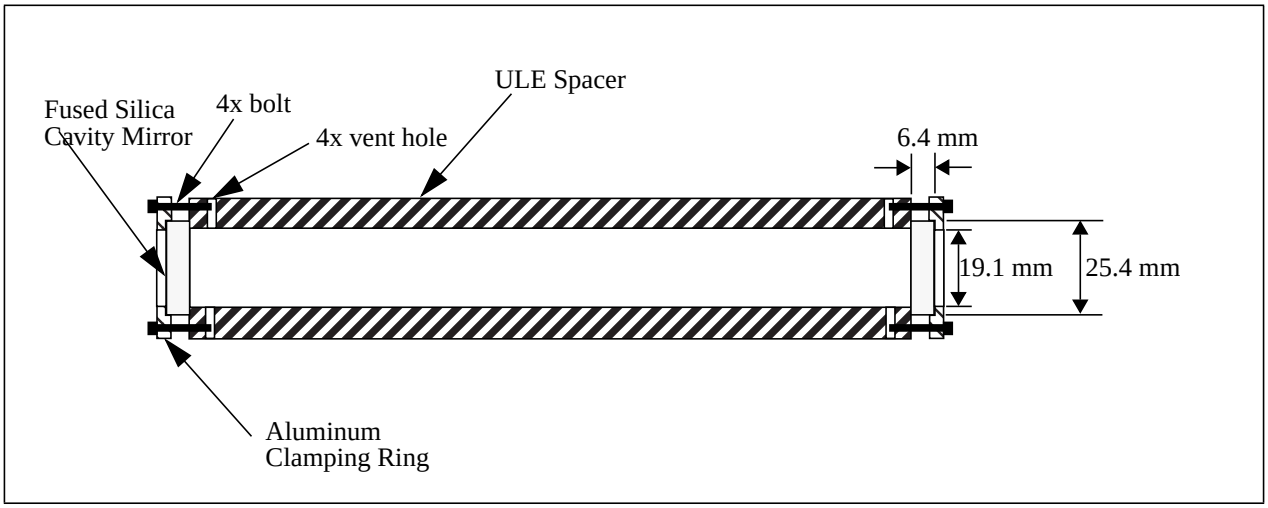

2 BOUNDARY CONDITIONS

The mirrors have a complex boundary condition. There is conductive contact between the mirror back face outer perimeter (and potentially part of the mirror cylindrical edge) and the aluminum clamping ring. The clamping ring in turn is in conductive contact with the cavity spacer through four bolts. The outer perimeter of the front face of the mirror is in conductive contact with the cavity spacer. The mirror front face is radiatively coupled to the cavity spacer interior. The mirror

1. The method was originally proposed by the Japanese TAMA project, adopted by Stanford's GW group and proposed for use on LIGO by Jordan Camp. The method has recently been demonstrated by J. Camp, T. Yarnez and D. Li at Caltech.

back face is radiatively coupled to the vacuum chamber. The mirror cylindrical side surface is radiatively coupled with the vacuum chamber, the aluminum clamping ring, the cavity spacer and the bolts used to retain the mirror.

Since we are principally interested in the thermoelastically induced deflection of the front surface of the mirror due to heating from a small laser beam (waist, w = 0.4 mm), the boundary conditions along the perimeter of the mirror are not very significant (as will be shown below). The boundary conditions have been approximated by two extreme cases:

1) radiative coupling from all surfaces of the mirror to an uniform ambient temperature environment (T_∞ = 293K)

2) clamping the mirror temperature to a nominal ambient temperature (293K) at the outer perimeter of the front and rear faces (where conductive contact to the cavity spacer and aluminum clamping ring occurs) and radiatively coupling to the ambient on the remaining surface of the mirror

The radiative boundary condition was linearized via a Taylor series expansion:

$$q_{rad} = \sigma\varepsilon(T^4 - T_\infty^4) \approx 4\sigma\varepsilon T^3(\Delta T) \equiv h_c(\Delta T) \quad (1)$$

where:

q_{rad} = net radiative flux from the surface

σ = the Stefan-Boltzman constant (= 5.67 x 10^8 W/m^2/K^4)

ε = surface emissivity (conservatively set equal to unity due to lack of a better value for the high reflectance coating on the fused silica substrate)

T = surface temperature

T_∞ = ambient temperature

$\Delta T = T - T_\infty$

h_c = effective heat transfer coefficient

3 FINITE ELEMENT MODEL

A steady-state, linear heat transfer analysis was performed using SDRC's I-DEAS Master Series 4 software. The finite element model is comprised of 3840 solid, linear brick elements. The discretization is finer in the central part of the mirror; There are 2880 elements within the central 4.8 mm diameter cylinder. The element size was linearly varied from the perimeter of this central region to the center by a factor of 20 in both the radial and longitudinal directions (element radial dimension varied from 500 to 25 μm). The finite element mesh is shown in Figure 2.

The gaussian intensity of the laser beam is imposed via a data surface defined over the central region (r < R/5, where R = the mirror outer radius). The laser absorbed radiant intensity is defined as:

$$I(r) = \left(\frac{2P}{\pi w^2}\right) e^{-2\left(\frac{r}{w}\right)^2} \quad (2)$$

Figure (2) Finite element model mesh

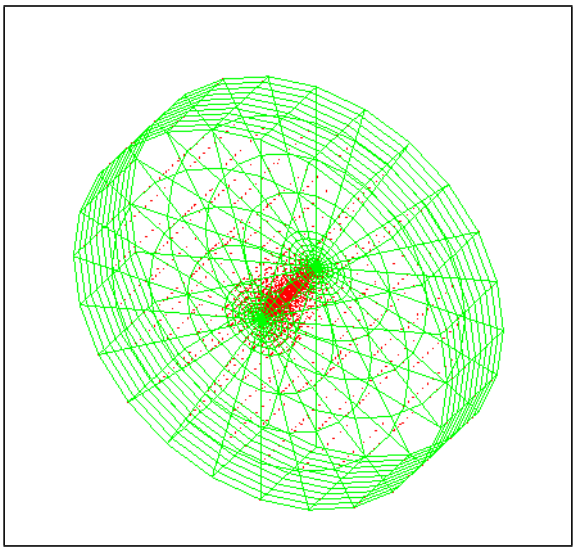

where:

P = absorbed power (W)

w = beam waist (i.e. the radius where the field amplitude is 1/e) (m)

The beam waist in the LIGO optical surface absorption/contamination measurement system is 0.4 mm.

4 RESULTS

All results are for an absorbed power, P = 1 Watt; Since the problem is linear for small temperature changes, the results can be scaled for other incident or absorbed power conditions. The displacement profile (exaggerated for the purpose of display) is shown in Figure 3.

Figure (3) Displacement profile and contour.

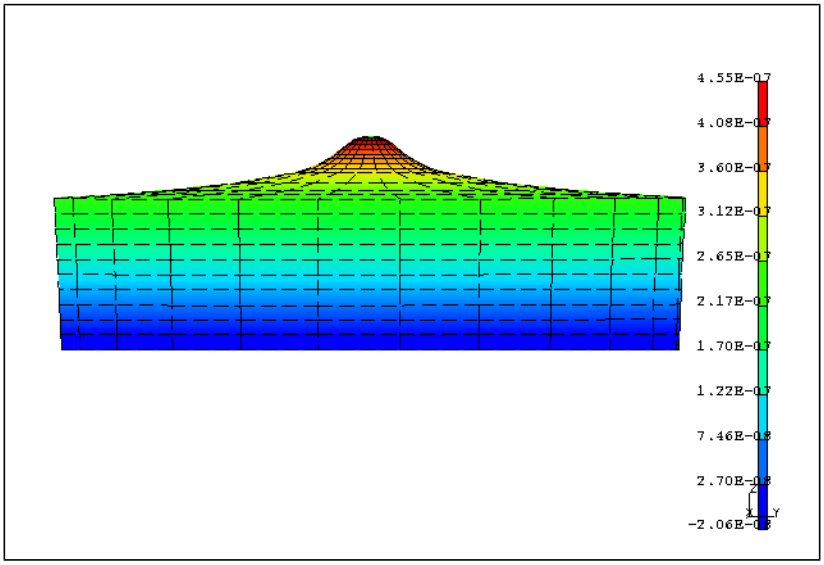

The temperature contours and diametrical plots, T(r=x), are shown in Figure 4. For boundary condition [1], radiation on all surfaces, the peak temperature rise above the ambient is 700 K/W; For boundary condition [2], with an outer annular perimeter of the front and rear faces clamped to the ambient temperature, the peak temperature rise above the ambient is 585 K/W.

Figure (4) Surface temperature rise (above ambient)

Temperature Contour	T(x)
[1] Radiation from all surfaces:	
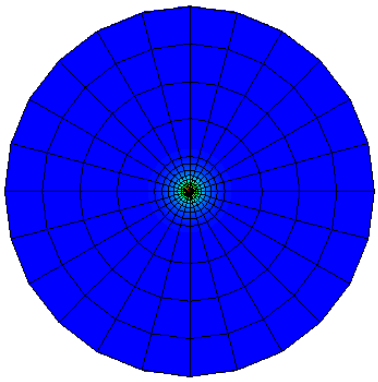	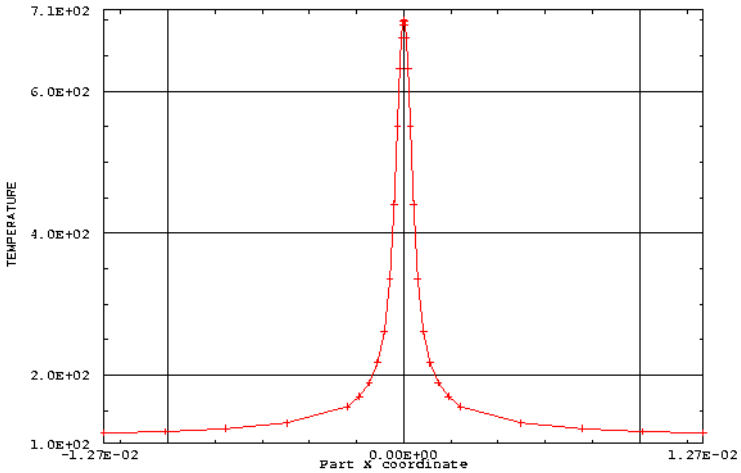
[2] Outer perimeter of faces clamped to ambient, other surface areas radiate:	
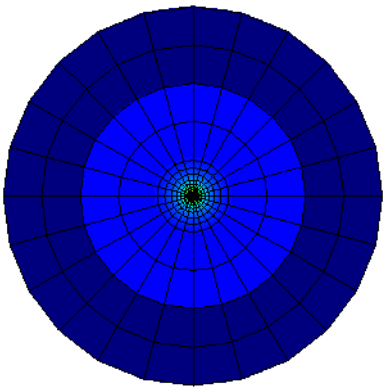	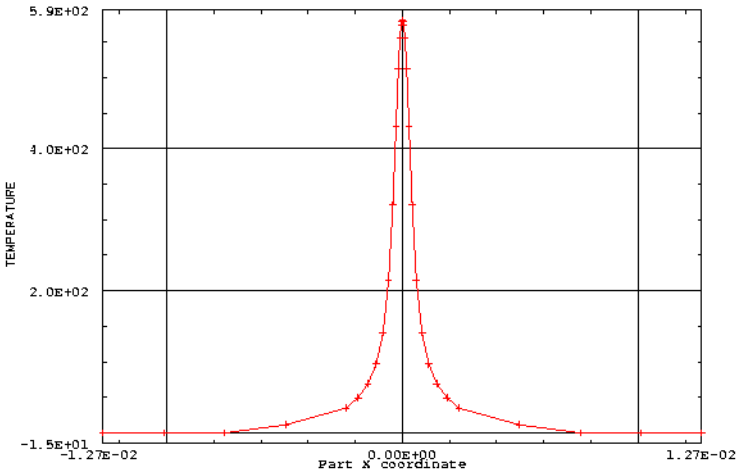

The displacement of the mirror front surface (in the direction normal to the surface) as a function of radius, $\delta(r)$, is shown in Figure 5 for boundary condition [1], all radiative surfaces and in Figure 6 for boundary condition [2], with the outer perimeter of the front and rear faces clamped to the

ambient temperature. The sagitta at r = w is 26 nm for both of the boundary conditions, i.e. the details of the outer perimeter boundary condition of the mirror does not influence the thermoelastic response of the region immediately under the laser beam. The mirror deflection is to first order well approximated by an effective radius of curvature change for r ~ w.

A simple approximate analysis[1] of the thermoelastic, steady-state deflection yields the same result:

$$\delta = \frac{\alpha P}{4\pi\kappa} \tag{3}$$

where (properties are given at 293K):

α = thermal coefficient of expansion for fused silica = 0.42 ppm/K
κ = thermal conductivity of fused silica = 1.38 W/m/K
or δ/P = 24 nm.

1. W. Winkler, et. al., “Heating by optical absorption and the performance of interferometric gravitational-wave detectors”, Physical Review A, vol. 44, No. 11, 1 Dec 91.

Figure (5) Displacement, δ(x) for boundary condition [1]: Radiation from all surfaces

Displacement, δ(x) for -r<x<r

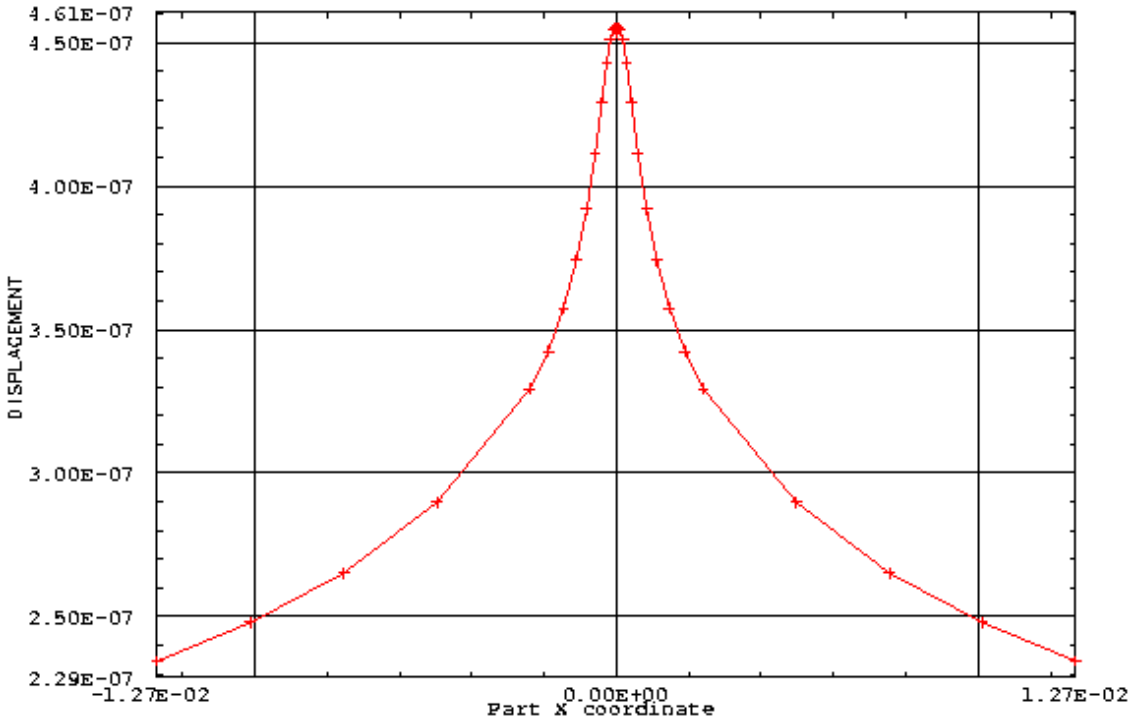

Displacement, δ(x) for -r/5<x<r/5

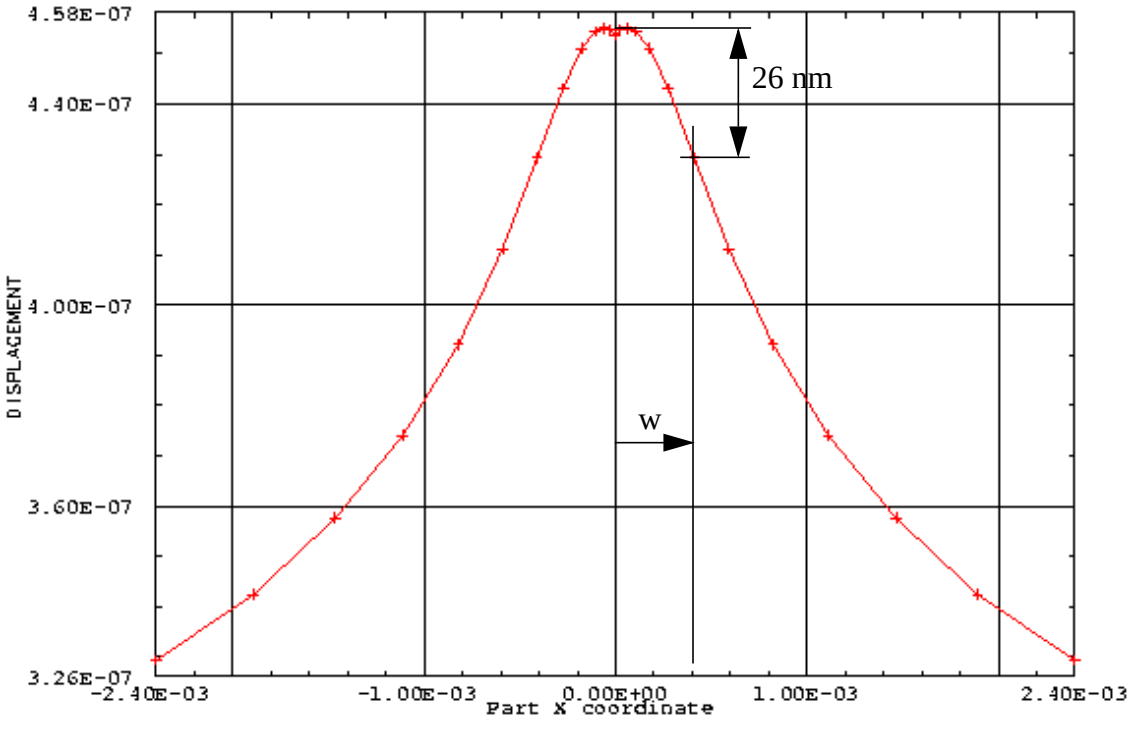

Figure (6) Displacement, δ(x) for boundary condition [2]:
Outer perimeter of faces clamped to ambient, other surface areas radiate

Displacement, δ(x) for -r<x<r

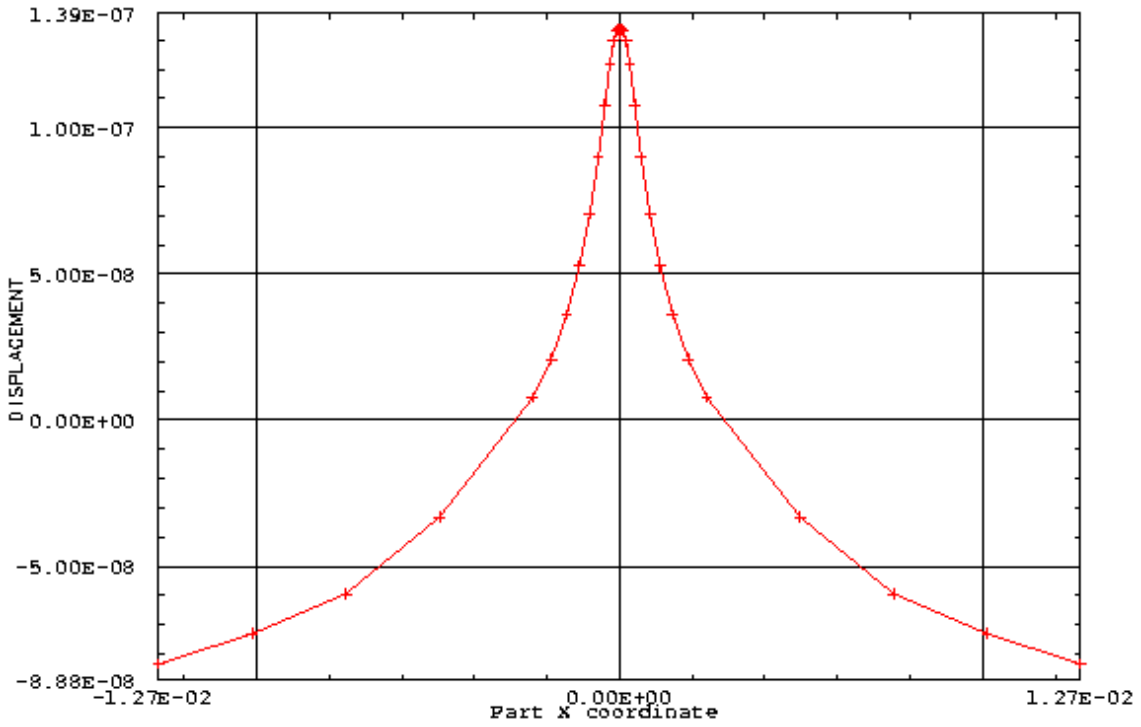

Displacement, δ(x) for -r/5<x<r/5